An Observational, Irrigation-Sensitive Agricultural Drought Record from Weather Data

LOIS I. TANG[a] AND KAIGHIN A. MCCOLL[a,b]

[a] Department of Earth and Planetary Sciences, Harvard University, Cambridge, Massachusetts
[b] School of Engineering and Applied Sciences, Harvard University, Cambridge, Massachusetts

(Manuscript received 10 February 2023, in final form 11 July 2023, accepted 16 August 2023)

ABSTRACT: The historical rise of irrigation has profoundly mitigated the effect of drought on agriculture in many parts of the United States. While irrigation directly alters soil moisture, meteorological drought indices ignore the effects of irrigation, since they are often based on simple water balance models that neglect the irrigation input. Reanalyses also largely neglect irrigation. Other approaches estimate the evaporative fraction (EF), which is correlated with soil moisture under water-limited conditions typical of droughts, with lower values corresponding to drier soils. However, those approaches require satellite observations of land surface temperature, meaning they cannot be used to study droughts prior to the satellite era. Here, we use a recent theory of land–atmosphere coupling—surface flux equilibrium (SFE) theory—to estimate EF from readily available observations of near-surface air temperature and specific humidity with long historical records. In contrast to EF estimated from a reanalysis that largely neglects irrigation, the SFE-predicted EF is greater at irrigated sites than at nonirrigated sites during droughts, and its historical trends are typically consistent with the spatial distribution of irrigation growth. Two sites at which SFE-predicted EF unexpectedly rises in the absence of changes in irrigation can be explained by increased flooding due to human interventions unrelated to irrigation (river engineering and the expansion of fish hatcheries). This work introduces a new method for quantifying agricultural drought prior to the satellite era. It can be used to provide insight into the role of irrigation in mitigating drought in the United States over the twentieth century.

SIGNIFICANCE STATEMENT: Irrigation grew profoundly in the United States over the twentieth century, increasing the resilience of American agriculture to drought. Yet observational records of agricultural drought, and its response to irrigation, are limited to the satellite era. Here, we show that a common measure of agricultural drought (the evaporative fraction, EF) can be estimated using widespread weather data, extending the agricultural drought record decades further back in time. We show that EF estimated using our approach is both sensitive and specific to the occurrence of irrigation, unlike an alternative derived from a reanalysis.

KEYWORDS: Atmosphere; North America; Drought; Soil moisture

1. Introduction

The irrigated area in the United States grew from 3 million acres in 1890 to more than 58 million acres in 2017, with half of that growth occurring after the 1950s (Hrozencik and Aillery 2021; McLeman et al. 2014). This profound growth has increased the resilience of American agriculture to drought. It also complicates the study of long-term changes in drought due, for example, to climate change, since even if droughts are becoming more severe, the rise of irrigation may result in a perception that they are less severe. For example, while the Dust Bowl drought of the 1930s is well known, droughts of arguably comparable magnitude have occurred several times in the United States since then, with much less acknowledgment: for example, the Texas drought of the 1950s (Woodhouse and Overpeck 1998; Worster 2004; Seager et al. 2005; Cook et al. 2007). The cooling effects of irrigation can also mask rises in near-surface air temperatures (Lobell and Bonfils 2008; Mueller et al. 2016; Nocco et al. 2019).

Droughts are extended periods of anomalously dry conditions. Periods of anomalously low precipitation are termed "meteorological droughts"; and periods of anomalously low soil moisture are termed "agricultural droughts." Clearly, the occurrence of these two types of drought are related. However, in irrigated regions, they can be disconnected: even if there is anomalously low rainfall for an extended period (a meteorological drought), an irrigated region will not necessarily experience anomalously low soil moisture (an agricultural drought). For example, Lu et al. (2020) reported lower sensitivity of crop yields to meteorological drought in irrigated regions compared to nonirrigated regions.

The distinction between meteorological and agricultural droughts is often blurred. For example, the Palmer drought severity index (PDSI; Palmer 1965) is a conventional index used to estimate the severity of droughts. In its calculation, precipitation and temperature data are processed through

Denotes content that is immediately available upon publication as open access.

Supplemental information related to this paper is available at the Journals Online website: https://doi.org/10.1175/JHM-D-23-0026.s1.

Corresponding author: Lois I. Tang, loistang@fas.harvard.edu

DOI: 10.1175/JHM-D-23-0026.1

an empirical water balance model, in a way that can appear superficially related to soil moisture, and thus agricultural drought. However, the PDSI is, at best, a highly ambiguous measure of agricultural drought (Alley 1984), and is better suited for studying meteorological drought. Indeed, the original report introducing the PDSI is entitled "Meteorological Drought" (Palmer 1965). Dai et al. (2004) noted that "the PDSI is an approximate measure of the cumulative effect of *atmospheric* moisture supply and demand (i.e., meteorological droughts) … we emphasize that, by design, the PDSI is not always a good measure of soil moisture and thus agricultural droughts" (italics in original). In cases where agricultural drought and meteorological drought are strongly correlated, the PDSI (and similar indices of meteorological drought) may still provide useful information on agricultural drought. But, in regions where irrigation is an important component of the soil water balance, agricultural drought and meteorological drought can be entirely uncorrelated. For these reasons, we argue that the meteorological drought indices are unsuitable tools for quantifying the impacts of irrigation on agricultural drought severity.

What should be used instead? Ideally, long-term observations of soil moisture. However, soil moisture observations are spatially sparse (Vicente-Serrano et al. 2012), and the satellite record does not extend far enough back in time to study some of the most important droughts in the historical record (e.g., the Dust Bowl or the 1950s drought). Here, we consider a quantity that is strongly correlated with soil moisture, at least during water-limited conditions typical of droughts: the evaporative fraction (EF), the ratio of latent heat flux to total surface turbulent fluxes. EF increases with increasing water availability in water-limited regions, to the extent that it is often modeled conceptually as a simple function of (normalized) soil moisture (e.g., Koster et al. 2009; Seneviratne et al. 2010; Koster and Mahanama 2012). In irrigated regions, CMIP6 models with irrigation schemes—compared to models without irrigation schemes—better reproduced anomalies of surface fluxes in observations (Al-Yaari et al. 2022), further supporting the notion that the EF is sensitive to irrigation.

However, like soil moisture, observations of the surface fluxes needed to estimate EF also have limited spatial and temporal coverage. For this reason, a range of approaches exist in the literature for estimating variants of the EF. For example, the evaporative stress index (ESI; Anderson et al. 2011)—the ratio between actual and potential evapotranspiration retrieved from the Atmosphere–Land Exchange Inverse (ALEXI; Anderson et al. 1997) surface energy balance model—is an agricultural drought index based on observational land surface temperature that contains effects of irrigation and other factors decoupled from precipitation (Anderson et al. 1997, 2011). While these approaches are useful for studying drought in the present and the recent past, they cannot be used to understand droughts prior to the advent of the satellite record, since they require, at minimum, observations of land surface temperature and surface radiation (AghaKouchak et al. 2015). Historical observations of surface radiation do not exist prior to the satellite era. In addition, weather stations have historically measured near-surface air temperature rather than land surface temperature. This difference is not trivial: assuming surface temperature and near-surface air temperature are identical is equivalent to assuming that the sensible heat flux is zero, which implies that EF = 1 everywhere. That assumption is clearly inappropriate over land. Thus, current approaches for estimating EF cannot be used to study agricultural droughts occurring earlier than the satellite record.

In this study, we estimate EF from widespread weather data using surface flux equilibrium (SFE) theory (McColl et al. 2019; McColl and Rigden 2020). SFE takes advantage of the fact that wetter regions, with higher values of EF, exhibit greater evaporation, which causes the near-surface atmospheric humidity to be relatively high. Similarly, higher values of EF correspond to lower surface sensible heat fluxes, which causes near-surface atmospheric temperatures to be relatively low. SFE uses these hypotheses to estimate EF solely using near-surface weather data (temperature and humidity) and does not require information on land surface variables, including soil moisture, or calibration of site-specific parameters. Crucially, the SFE estimate of EF should, in principle, be sensitive to irrigation, without requiring explicit information on irrigation. The SFE theory has been extensively validated (McColl and Rigden 2020; Chen et al. 2021) and shown to perform well in water-limited regions and in the continental United States. It has also been used to successfully estimate root-zone soil moisture (Raghav and Kumar 2021). Since SFE hypothesizes that nonlocal advective fluxes of moisture and heat are typically small compared to local surface fluxes, it is an inappropriate tool in regions in which this assumption is strongly violated, such as near coastlines. However, the SFE hypothesis appears to work well in much of the inland United States (McColl and Rigden 2020; Chen et al. 2021), which is the focus of this study, despite the presence of land surface heterogeneity and associated advection in these regions. The major advantage of SFE over previous approaches based on evaporation is that it is capable of estimating EF using available weather station data (near-surface air temperature and specific humidity). This means that it can be used to study agricultural drought prior to the satellite era, unlike previous approaches.

In this study, we will show empirically that EF estimated using SFE is sensitive and specific to irrigation, in contrast to an estimate from a reanalysis that largely neglects irrigation. Because the theory only requires near-surface air temperature and specific humidity as inputs and does not require site-specific calibration, the agricultural drought record can, in principle, be extended as far back as the meteorological record allows, opening up new opportunities for understanding drought in the twentieth century.

The manuscript is structured as follows. In section 2, we describe the data used in this study and how they are analyzed. Section 3 presents results of analyses of data from the present and the historical record. In section 4, we summarize the study's main findings and discuss its limitations and possible future applications.

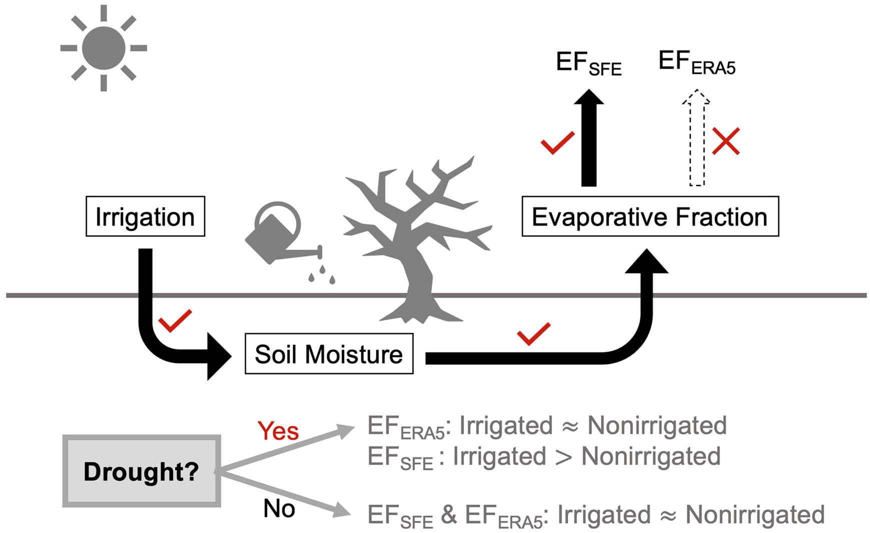

FIG. 1. Schematic overview of this study. During meteorological droughts, over irrigated regions, soil is moistened by irrigation, which leads to a higher local evaporative fraction. While EF_{SFE} is sensitive to this shift in soil moisture state, EF_{ERA5} is not. Thus, if there is a meteorological drought, we expect EF_{SFE} in irrigated regions to be higher than nonirrigated regions, but not EF_{ERA5}. In contrast, when there is no drought, the two drought indices at different regions should both be insensitive to irrigation.

2. Methods

a. Analysis rationale

We aim to test the hypothesis that SFE-estimated EF (EF_{SFE}) is sensitive and specific to irrigation, whereas an estimate derived from the ERA5 reanalysis (EF_{ERA5}) that largely neglects irrigation is not. To do this, we seek to compare EF_{SFE} and EF_{ERA5} at irrigated and nonirrigated points in space and time and identify systematic differences between the two quantities during droughts. After correcting for other confounding factors, the remaining differences are attributable to irrigation. Testing this hypothesis is complicated by the fact that long-term irrigation data are limited. Estimation of irrigation water withdrawal by hydrological models is unreliable (Puy et al. 2022), and irrigation data are certainly not available at the spatial and temporal resolution of the weather and reanalysis data. Thus, our analysis is structured around the temporal and spatial scale and coverage allowed by available irrigation data.

The analysis rationale is summarized in Fig. 1. In a meteorological drought, irrigation reduces the deficit in soil moisture. Since the ERA5 reanalysis does not include irrigation, we expect that EF_{ERA5} will still predict a drought even though irrigation has replenished soil moisture. In contrast, we expect that EF_{SFE} will not predict a drought in irrigated regions, since EF_{SFE} is sensitive to the influence of irrigation on air temperature and humidity. When there is no meteorological drought, we do not expect there to be systematic differences between the two quantities. More specifically, we test the following hypotheses:

1) H1. During periods of meteorological drought, EF_{SFE} is greater at irrigated sites, compared with nonirrigated sites.
2) H2. Outside periods of meteorological drought, there are negligible differences in EF_{SFE} between irrigated and nonirrigated sites.
3) H3. Both during, and outside of, periods of meteorological drought, there are negligible differences in EF_{ERA5} between irrigated and nonirrigated sites.
4) H4. In regions where irrigation has increased with time, EF_{SFE} has also increased during meteorological droughts, relative to EF_{ERA5}.
5) H5. In regions where irrigation has not increased with time, there are negligible changes in EF_{SFE} during meteorological droughts, relative to EF_{ERA5}.

Hypotheses H1, H2, and H3 test the sensitivity and specificity of EF_{SFE} to irrigation variability in space. Hypotheses H4 and H5 test the sensitivity and specificity of EF_{SFE} to irrigation variability in time.

b. Evaporative fraction

The evaporative fraction is the ratio between surface latent heat flux and the sum of latent heat and sensible heat fluxes. In water-limited conditions typical of agricultural droughts, the EF is an approximately linear increasing function of soil moisture (Koster et al. 2009; Seneviratne et al. 2010; Koster and Mahanama 2012). Various approaches exist for estimating EF using satellite observations (Anderson et al. 1997, 2011; AghaKouchak et al. 2015). Estimating EF prior to the satellite era requires a different approach, detailed in the following section.

1) ESTIMATION OF EF USING SFE THEORY

We briefly review SFE, a phenomenological theory of evapotranspiration used in this study, but refer the reader to

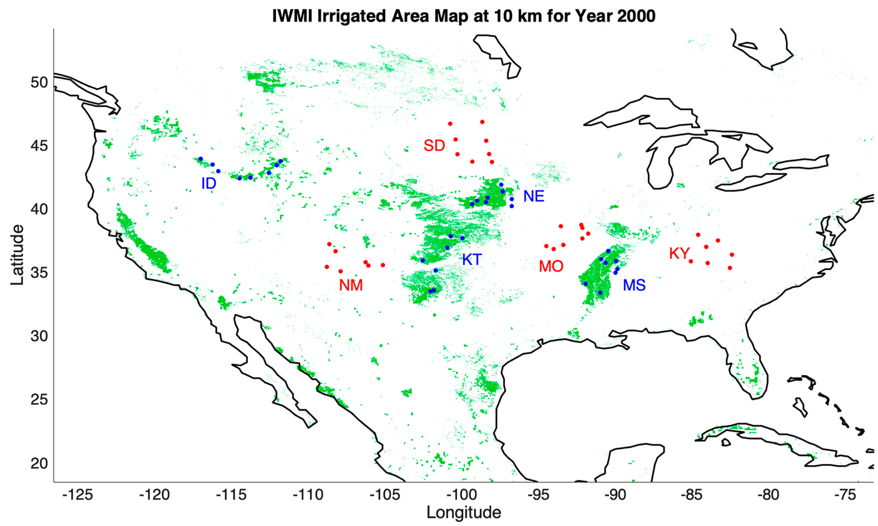

FIG. 2. The International Water Management Institute (IWMI) 10-km irrigation area map in 2000 (https://waterdata.iwmi.org/Applications/GIAM2000/), with irrigated regions marked in green. Sites from the HadISD database located in irrigated regions are marked in blue; sites from nonirrigated regions are marked in red. Clusters of irrigated sites are grouped into ID (Idaho region), NE (Nebraska), MS (around the Mississippi River), and KT (Kansas and Texas); clusters of nonirrigated sites are grouped into NM (New Mexico), SD (South Dakota), MO (Missouri), and KY (Kentucky).

McColl et al. (2019) and McColl and Rigden (2020) for further details. The near-surface atmospheric state is sensitive, to some degree, to surface fluxes. Thus, higher near-surface air temperatures are at least partly caused by higher surface sensible heat fluxes; and higher values of near-surface specific humidity are partly caused by higher surface latent heat fluxes. If the near-surface atmospheric state is sufficiently sensitive to surface fluxes, then the surface moistening and heating terms in the near-surface relative humidity budget approximately balance. SFE assumes a strong sensitivity of the near-surface atmospheric state to surface fluxes, and that the surface moistening and heating terms in the near-surface relative humidity budget exactly balance. This further implies that the evaporative fraction can be estimated using the relation

$$\mathrm{EF}_{\mathrm{SFE}} = \frac{\lambda^2 q_a}{\lambda^2 q_a + c_p R_v T_a^2},$$

where $\mathrm{EF}_{\mathrm{SFE}}$ is the SFE-predicted EF, $R_v = 461.5\ \mathrm{J\ kg^{-1}\ K^{-1}}$ is the gas constant of water vapor, $c_p = 1004\ \mathrm{J\ kg^{-1}\ K^{-1}}$ is the specific heat capacity of air, T_a is the near-surface air temperature (K), $\lambda = 2.5 \times 10^6\ \mathrm{J\ kg^{-1}}$ is the latent heat of vaporization, and q_a is the near-surface specific humidity ($\mathrm{kg\ kg^{-1}}$).

The main advantage of SFE over other approaches is its simplicity: unlike most approaches, it requires no land surface information and no tuning of calibration parameters. This is particularly important for our purposes, since we are interested in past droughts for which it is rare to have direct observations of land surface variables, such as soil moisture, which are essential inputs to other models of EF. Its use is not recommended in coastal regions, where the assumptions of SFE are expected to be strongly violated by land–sea breeze mesoscale circulations. It also underestimates EF somewhat for particularly high values of EF, and overestimates it for low values, resulting in a compressed dynamic range [similar behavior is also found in other approaches, e.g., Salvucci and Gentine (2013)]. Nevertheless, despite these caveats and SFE's simplicity, it is surprisingly accurate, with errors comparable to those in state-of-the-art eddy covariance observations (McColl and Rigden 2020) and lower than those in a complex reanalysis (Chen et al. 2021) across a wide range of conditions in inland continental regions.

2) HadISD site-level data

The HadISD global subdaily station dataset v3.1.0.2019f (Dunn et al. 2016) includes observations of temperature and humidity from the 1930s to the present across the continental United States (CONUS) region. We use site-level (i.e., not gridded) temperature and humidity data to estimate EF using the SFE theory. Using the global irrigated area map at 10 km resolution in 2000 from the International Water Management Institute (IWMI; Thenkabail et al. 2009), we selected four groups of irrigated sites and four groups of nonirrigated sites from the full set of HadISD sites in the CONUS region (Fig. 2). The four irrigated regions are located in Idaho's Snake River basin (ID), Nebraska (NE), the Great Plains region of Kansas and Texas (KT), and the lower Mississippi River basin (MS). We did not include the Central Valley in California due to the fact that it is close to the coast, where the assumptions of SFE are likely strongly violated (McColl and Rigden 2020). Although two NE sites and two MS sites are located in counties with relatively low irrigation rates, the elimination of those

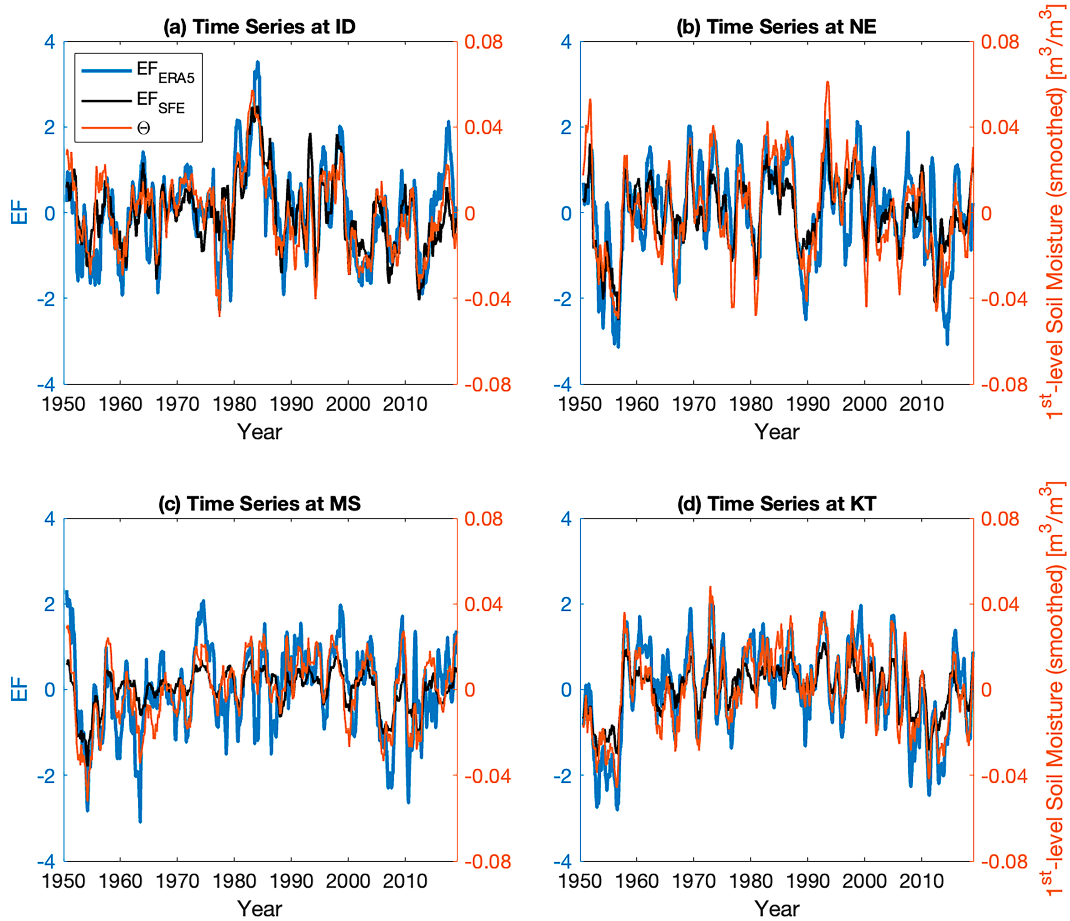

FIG. 3. Long-term consistency between EF_{SFE} (black), EF_{ERA5} (blue), and 13-month-smoothed normalized anomalous soil moisture in ERA5 (Θ, red) from 1950 to 2018. The sites are the four irrigated sites: (a) ID, (b) NE, (c) MS, and (d) KT. Qualitatively similar results are found at the nonirrigated sites (not shown).

four sites does not qualitatively change any of the results in this study (not shown). The four nonirrigated regions are located in the region west of KT (around New Mexico, hereafter NM), the region north of NE (around South Dakota, hereafter SD), the region between KT and MS (around Missouri, hereafter MO), and the region east of MS (around Kentucky, hereafter KY). Among all the HadISD sites in the irrigated and nonirrigated areas, we each selected seven or eight sites that 1) had complete and valid meteorological observational data extending to at least 1973 if possible and 2) were within 500 km of other sites in the same group. Please refer to Tables S1 and S2 in the online supplemental material for the location and temporal coverage of the selected sites.

While EF is approximately linearly related to soil moisture under water-limited conditions typical of droughts, the parameters of the linear relation vary in space. To more easily make spatial comparisons, we consider anomalies of EF relative to the mean estimated over the period 1950–2018 (the longest window of time that overlaps with ERA5 reanalysis data), calculate the 13-month moving average, and normalize by the standard deviation at each site. For brevity, we do not introduce new notation for normalized anomalies: for the remainder of the manuscript, any reference to EF_{SFE} or EF_{ERA5} refers to a normalized anomaly. When generating time series of the SFE-predicted EF anomaly (EF_{SFE}), missing data were neglected when calculating moving averages. The estimated anomalies correlate reasonably well with both anomalies of EF estimated using the ERA5 reanalysis (EF_{ERA5}) and soil moisture from the reanalysis (Fig. 3).

3) ERA5 REANALYSIS DATA

We also include estimates of EF obtained from the ECMWF ERA5 reanalysis data (Hersbach et al. 2020). To compare this gridded reanalysis dataset with site-level data, we also generated averages of each group based on the gridded location of HadISD sites. Anomalies were estimated in the same way as for the HadISD site-level data.

While site-level observations and reanalysis both include climatic and meteorological factors, the most relevant difference between EF_{SFE} and EF_{ERA5} is that the land-use distribution of EF_{ERA5} does not evolve with time. Long-term influences on EF from changes in human activity such as irrigation, river engineering, and other hydrologic construction projects are not explicitly included in ERA5. ERA5 does assimilate some near-surface air temperature and humidity data, but it is highly limited in spatial coverage (Hersbach et al. 2020). It also assimilates some C-band scatterometer soil moisture retrievals (Hersbach et al. 2020), but they only sense moisture in a very shallow layer of soil and are less accurate than other soil moisture retrievals (Chen et al. 2018). Thus, using EF_{ERA5} helps us 1) verify the overall consistency with EF_{SFE} in different regions and 2) isolate the effect of human activities, by comparing EF_{ERA5} with EF_{SFE}.

c. Irrigation data

The United States Department of Agriculture (USDA) has county-level irrigated area census data dating back to 1974 (USDA National Agricultural Statistic Service 2022). The census was taken every 4–5 years. We estimated trends in irrigated areas in different site groups by calculating the proportion of irrigated area in the counties where the sites are located (counties listed in Tables S1 and S2).

To best investigate the effects of irrigation, we focus on the growing season—May–September (MJJAS)—in all of our analyses.

d. Palmer drought severity index

Outside irrigated areas, meteorological and agricultural droughts often occur together. We use the PDSI to classify periods of meteorological drought in this study, for consistency with previous studies. The PDSI is generated using precipitation and temperature data as inputs into a water-balance model (Palmer 1965; Alley 1984). We use monthly gridded PDSI data (Dai et al. 2004). The spatial resolution of the data is 2.5° latitude × 2.5° longitude. The dataset is available from 1948 to 2014. This is longer than the available record of county-level irrigation census data (USDA National Agricultural Statistic Service 2022), so we focus on the period 1974–2012.

The PDSI indicates drier than normal conditions when it is negative. The threshold of PDSI that determines the onset of a drought is somewhat arbitrary. In testing hypotheses H1 and H2, we adopt the same convention as the U.S. Drought Monitor, which uses a threshold of PDSI ≤ -2 for its definition of a drought. That threshold also corresponds to the threshold for a "moderate drought" proposed in Palmer's original report (see Table 11 of Palmer 1965). We use the threshold PDSI > 0 to identify periods that are not in drought, again consistent with the U.S. Drought Monitor and Palmer's original report. In testing hypotheses H4 and H5, we would ideally like to use the same thresholds. However, we are not able to do this due to limits on the analyses' temporal window imposed by the irrigation data, which result in insufficient sample sizes when a threshold of PDSI ≤ -2 is used (described further in section 3b). As a compromise between these considerations, we use a threshold of PDSI < 0 to define a drought in testing hypotheses H4 and H5. While not ideal, this definition is at least consistent with conditions being drier than average. For both sets of analyses, we investigate the sensitivity of our analyses to these choices of thresholds.

e. Significance testing

We use Student's t tests to evaluate the hypotheses H1–H5 listed earlier in section 2a. More precisely, for each hypothesis H1–H5, we test the complementary null hypotheses $H1_0$–$H5_0$: for example, for H1, the complementary null hypothesis $H1_0$ is "During periods of meteorological drought, EF_{SFE} is no greater at irrigated sites, compared with nonirrigated sites." The estimated p value is the probability of observing the data, assuming the null hypothesis is true. If the p value is sufficiently small—where a common choice of "sufficiently small" is taken to be $p < 0.05$—then we may reject the null hypothesis, in which case the result is significant at the 95% level.

However, if multiple significance tests are conducted, it becomes increasingly likely that a statistically significant result will arise spuriously due to chance (Wilks 2016). To correct for this, we control the "false discovery rate" using the approach of Benjamini and Hochberg (1995), recommended in Wilks (2016) [see their Eq. (3)]. After making these corrections, the appropriate threshold for statistical significance is lower than 0.05. To avoid confusion, rather than reporting the p value for each statistical test, throughout the manuscript, we simply report results as being statistically significant or insignificant.

Since hypotheses H1–H3 specifically test whether or not EF is greater at irrigated sites than nonirrigated sites, one-tailed t tests were performed. For hypotheses H4 and H5, absolute temporal changes in EF may be positive or negative, even where irrigation has increased (e.g., due to changes in climate). We therefore perform two-tailed t tests for H4 and H5.

3. Results

In this section, we will first test spatial hypotheses H1–H3 using data from the "present": the period 2000–12. Then, we will test temporal hypotheses H4 and H5 using historical irrigation trends.

a. Present (2000–12)

Since our selections of irrigated and nonirrigated sites are based on the IWMI irrigated area map for the year 2000 (Fig. 2), we first compare all the available data during the growing season from 2000 to 2012. In Fig. 4, EF_{SFE} (top panel) and EF_{ERA5} (bottom panel) are plotted against PDSI. The scatterplots (Figs. 4b,e) show irrigated data in blue and nonirrigated data in red. Each dot indicates the mean value of a site in a certain month. Panels on the two sides show the distribution of EFs for times in which droughts occurred (Figs. 4a,d), and did not occur (Figs. 4c,f).

During meteorological droughts, EF_{SFE} is significantly larger over irrigated regions, compared with nonirrigated regions (Fig. 4a). This supports hypothesis H1. In contrast, outside periods of meteorological drought, values of EF_{SFE} in the irrigated and nonirrigated regions are not significantly different (Fig. 4c). This supports hypothesis H2. Consistent with hypothesis H3, there is no statistically significant difference in EF_{ERA5} between irrigated and nonirrigated regions, both

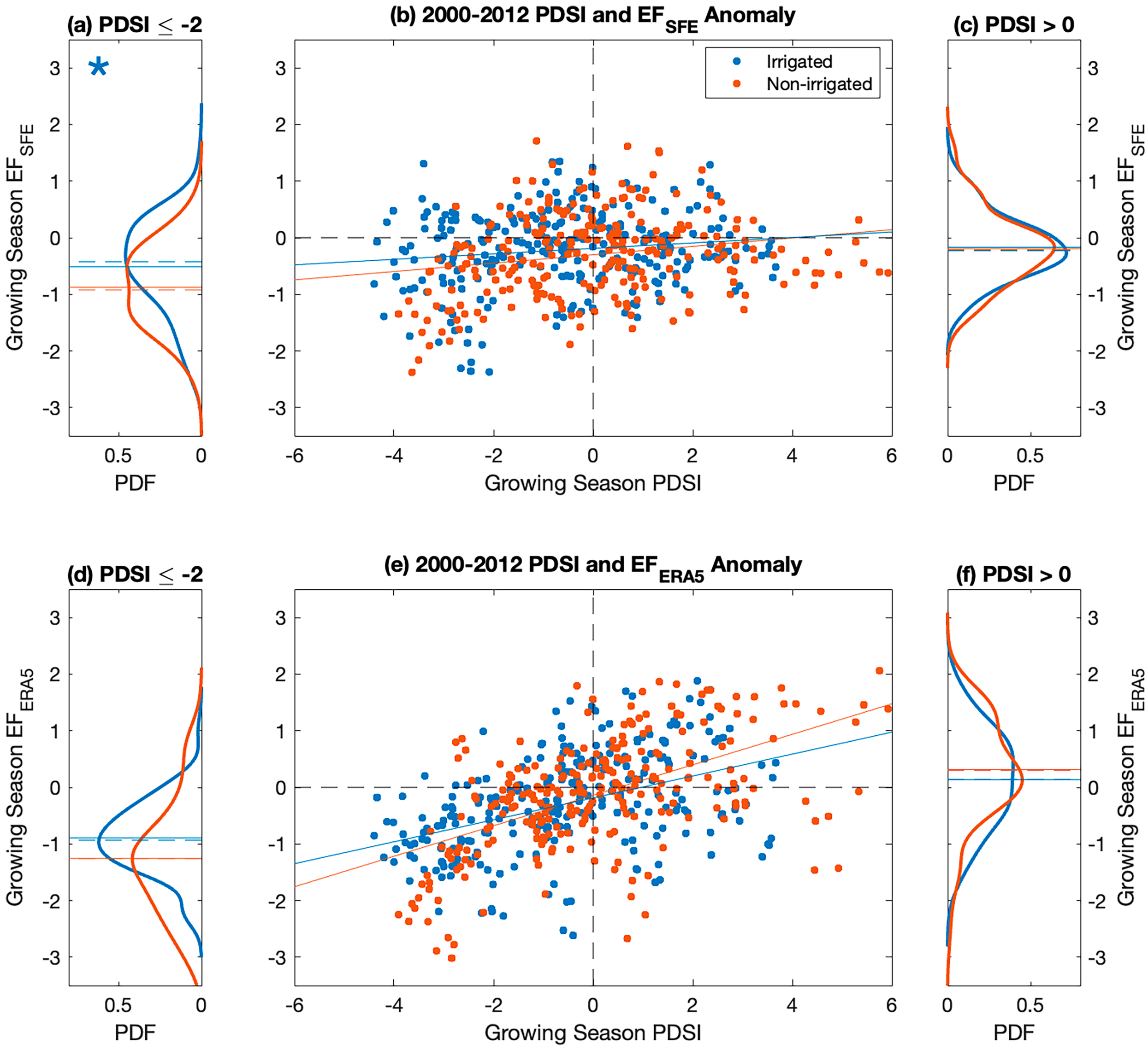

FIG. 4. (b) Scatterplot of PDSI and EF_{SFE} anomalies for the period 2000–12 at irrigated (blue) and nonirrigated (red) sites. (a) Probability density functions (PDFs) of EF_{SFE} at irrigated (blue) and nonirrigated (red) sites when PDSI ≤ -2 (corresponding to periods of drought). The solid and the dashed horizontal lines indicate the mean and median of the samples, respectively. The asterisk (*) indicates a statistically significant difference. (c) As in (a), but with PDSI > 0 (corresponding to periods that are not drought). (d)–(f) As in (a)–(c), but with EF_{ERA5} instead of EF_{SFE}.

during droughts (Fig. 4d), and outside periods of drought (Fig. 4f).

Our results are not particularly sensitive to reasonable variations in the PDSI threshold used here to define a drought. For example, changing the drought threshold from PDSI ≤ -2 to PDSI ≤ -1.5 does not change the results of the significance tests.

b. *Historical trends*

Next, we examine historical trends in irrigation. Both EF_{ERA5} and EF_{SFE} vary in time for reasons other than changes in irrigation (e.g., due to changes in climate). However, long-term changes in the difference between the two datasets should be due to processes that are not modeled in ERA5 but can still influence real-world EF. Such potential factors include irrigation and other hydrologic changes caused by humans.

To investigate hypotheses H4 and H5, we compared EF between two 13-yr windows: 1970–82 and 2000–12. Based on USDA county-level data for the area of irrigated land, we find increasing trends in irrigated area in MS, NE, and NM from 1974 to 2012 (Fig. 5). At MS, NE, and NM, the proportion of county irrigated increased at a rate of 8.75%, 4.19%, and 0.20% per decade, respectively ($p < 0.01$, using a Mann–Kendall test). Climatological and meteorological factors influence both

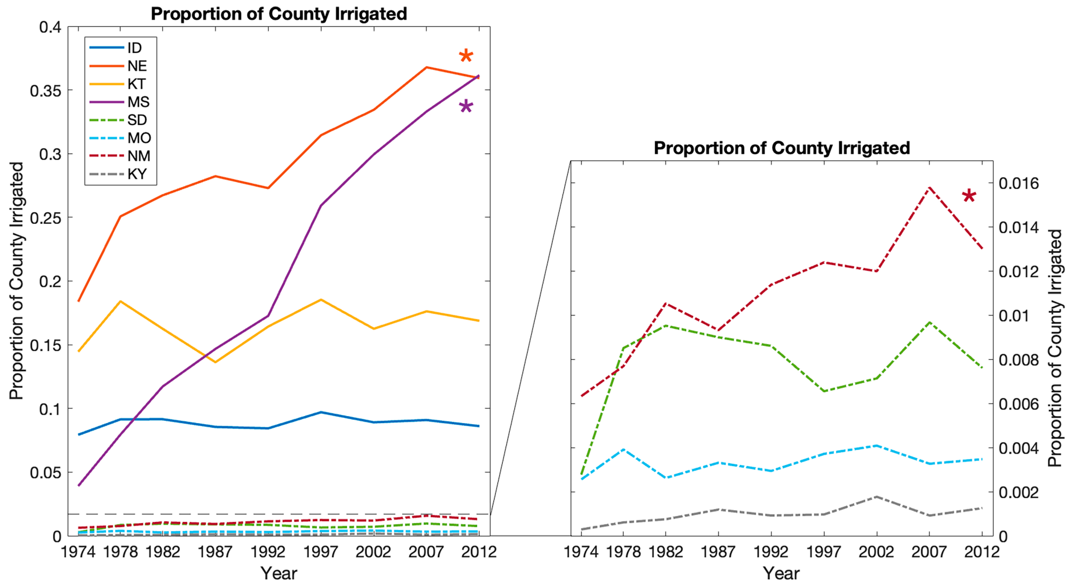

FIG. 5. Changes in irrigated area since 1974, based on the USDA census (conducted every 4 or 5 years). Data with asterisks (*) on the right indicate that both 1) there is a statistically significant monotonic increasing trend in irrigation in the county ($p < 0.01$), based on a Mann–Kendall test, and 2) at least 1% of the county is irrigated. (left) Proportion of county irrigated, based on USDA census data. Counties are listed in Tables S1 and S2. (right) As in the left panel, but zoomed in.

EF_{SFE} and EF_{ERA5}, but irrigation is only visible to EF_{SFE}. Thus, over the three regions with increasing trends in irrigated land, EF_{SFE} during meteorological droughts is expected to have increased, relative to changes in EF_{ERA5}.

As noted in section 2, use of the PDSI ≤ -2 drought threshold is precluded by low sample sizes when analyzing the historical data. This problem is illustrated in Fig. S1. For example, using a threshold of PDSI ≤ -2 would result in six out of eight sites having sample sizes less than $n = 3$, which is clearly insufficient. We thus use a threshold of PDSI < 0 to define a drought in testing hypotheses H3–H5 with the historical data, and examine the sensitivity of results to this choice.

The data at the three sites with increasing irrigation show an increase in EF_{SFE} relative to EF_{ERA5} during meteorologically dry periods. They are thus consistent with hypothesis H4. Figures 6 and 7 show EF_{SFE} and EF_{ERA5} in the two windows over regions with and without increasing trends in irrigation, respectively. Among the three sites that underwent an increase in irrigated land (Fig. 6), in NE, EF_{SFE} is significantly greater in 2000–12 than in 1970–82 (Fig. 6a), while EF_{ERA5} shows no significant difference between the two windows (Fig. 6d). In MS, EF_{SFE} is significantly greater in 2000–12 than in 1970–82 (Fig. 6b), in contrast to EF_{ERA5}, which does not change significantly (Fig. 6e). Finally, in NM, EF_{SFE} is not significantly greater in 2000–12 than in 1970–82 (Fig. 6c), but this is in contrast to EF_{ERA5}, which significantly decreased (Fig. 6f). This is consistent with an increase in EF_{SFE} relative to EF_{ERA5} in NM. Therefore, all three sites are consistent with H4.

Of the five remaining sites (all sites in which there was no appreciable rise in irrigation, Fig. 7), three of them are consistent with hypothesis H5, but two are not. At KT and KY, there is no significant increase in EF_{SFE} or EF_{ERA5} (Figs. 7b,e,g,j). At SD, both EF_{SFE} and EF_{ERA5} increase significantly, implying that changes in meteorology or climate are responsible for the change, rather than irrigation (Figs. 7c,h). These three sites are all consistent with hypothesis H5. However, the remaining two sites (MO and ID) are not. In both MO and ID, EF_{SFE} is significantly greater in 2000–12 than in 1970–82, while EF_{ERA5} is not (Figs. 7a,d,f,i).

Human modifications to local hydrology, other than irrigation, likely explain the anomalous observed responses at MO and ID. For the MO sites, we suggest that construction along the lower Missouri River has caused long-term changes in EF during droughts. The lower Missouri River has undergone significant engineering and construction programs, including some construction in the 1970s. A side effect of these changes has been an increased flood hazard in the region (Pinter and Heine 2005). Among the eight MO sites, if we eliminate two of the sites closest to the river, the results change from EF_{ERA5} showing no statistically significant increase, to showing a statistically significant increase (Fig. S2). There is no change to EF_{SFE}. Thus, eliminating the two sites closest to the river makes the results at MO consistent with hypothesis H5. The flooding induced by river engineering and construction at the MO sites is unique and not expected to occur at other sites. NE and KT depend on groundwater as the dominant source of irrigation, rather than surface water flow (Evett et al. 2020). For MS, although human activities influence the *magnitude* of flooding events, variations in the *frequency* of floods in the lower Mississippi River basin is dominated by climate variability and is thus consistent between ERA5 and observations (Munoz et al. 2018). At MO, river engineering was found to lower the flow

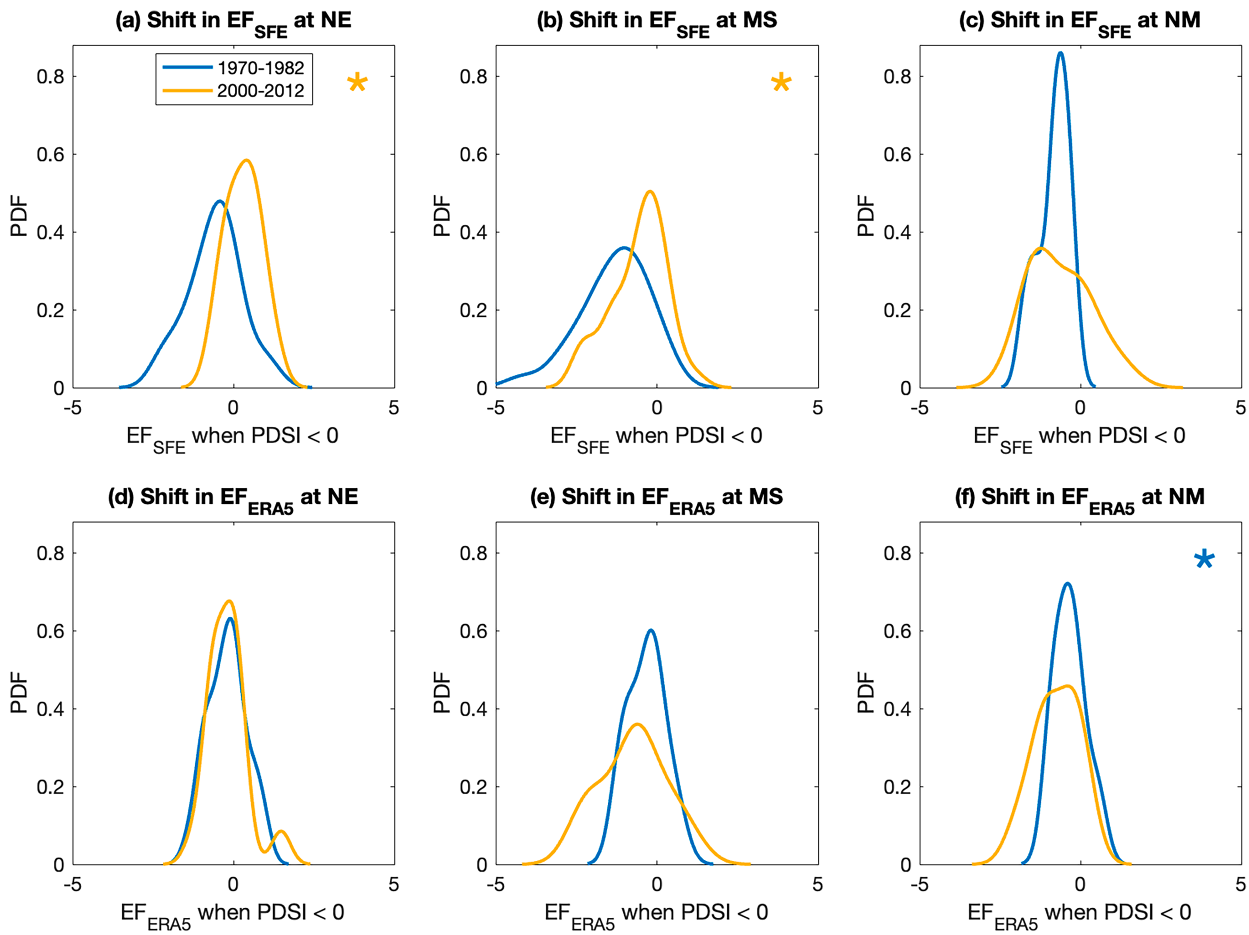

FIG. 6. Comparison between PDFs of the EF in 1970–82 (blue) and 2000–12 (yellow) when PDSI is negative for sites with increasing trends in irrigation since the 1970s as shown in Fig. 5. Panels with an asterisk (*) on the upper right indicate statistically significant differences, where the color of the asterisk indicates the period in which EF was greater. The panels correspond to results for (a),(d) NE; (b),(e) MS; and (c),(f) NM for (top) EF_{SFE} and (bottom) EF_{ERA5}.

capacity, which leads to floods even when the same amount of river flow would not lead to floods decades ago. In contrast, river engineering at MS was found to magnify the severity when there are flooding events in wet years, but there is no impact reported on flow capacity in normal or dry years, to our knowledge. Major flooding events around NM, SD, and KY are mostly contributed by flash flooding from storm events that are not related to river flow (flood information, National Weather Service: https://www.weather.gov/safety/flood-map). Although SD underwent some historical dam overflow events, the major dams in the region were constructed before the 1970s. To our knowledge, there is no elevated flood frequency due to river-related constructions reported at sites other than MO. We thus suggest that human activities regarding river engineering does not significantly contribute to the difference between the evolution in EF_{ERA5} and EF_{SFE} at other sites.

For ID, we suggest that expansion of fish hatcheries likely explains shifts in EF_{SFE} relative to EF_{ERA5} at ID sites. Along the irrigated valley in ID that we are interested in, there are four fish hatcheries, where three of them were under development in the 1970s and 1980s (Idaho Fish and Game 2022). Hagerman Hatchery was constructed in 1932 and renovated in 1979, Niagara Springs Hatchery was built in 1966 and renovated in 2013, Magic Valley Hatchery began operations in the late 1980s, and American Falls Hatchery was rebuilt during the mid-1980s. The construction of fish hatcheries in Idaho can alter the exposure of water to the atmosphere along the lower Snake River and contribute to changes in local EF. In the six sites that exhibit changes in EF_{SFE} relative to EF_{ERA5} in the past three decades consistent with our expectation, only SD is around national fish hatcheries. There are four major fish hatcheries in the region: the Garrison Dam National Fish Hatchery, Valley City National Fish Hatchery, DC Booth National Fish Hatchery, and Gavins Point National Fish Hatchery. However, to our knowledge, all four hatcheries appear to have completed construction before 1970 (U.S. Fish and Wildlife Service: https://www.fws.gov/). Thus, we suggest that the effects of fish hatchery construction is not an obviously significant factor in sites other than ID.

These results are reasonably insensitive to varying the PDSI < 0 drought threshold. Changing the threshold to

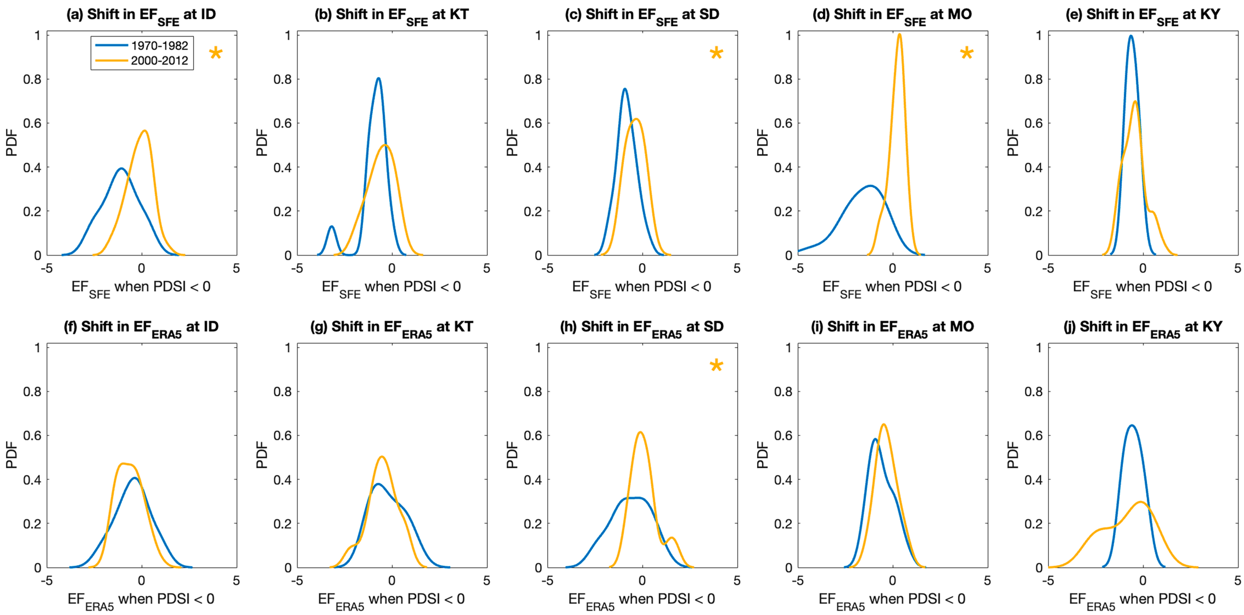

FIG. 7. As in Fig. 6, but for the other five sites without increasing trends in irrigation. Columns from left to right correspond to (a),(f) ID; (b),(g) KT; (c),(h) SD; (d),(i) MO; and (e),(j) KY.

PDSI ≤ -0.5 requires eliminating KY from the analysis, because the sample size becomes insufficient. Of the remaining seven sites, the conclusions are unchanged at six sites. The one exception occurs at SD, where EF_{SFE} no longer has a statistically significant change. As noted above, SD is a region where EF is influenced by human interventions unrelated to irrigation (fish hatcheries), a potentially confounding factor in the analysis.

4. Discussion and conclusions

The rise of irrigation has profoundly moderated the effect of drought on agriculture in many parts of the United States. We argue that meteorological drought indices and reanalysis proxies of soil moisture based on models without irrigation schemes (such as EF_{ERA5}) are insufficient to reflect the actual moisture conditions in irrigated regions. Current approaches based on the EF, a more direct measure of agricultural drought, are limited to the satellite era (AghaKouchak et al. 2015). In this study, we demonstrate that SFE theory can be used to estimate EF from widely available weather data with a long historical record. EF_{SFE} is a useful measure of agricultural drought that is sensitive and specific to irrigation and can be used to study droughts prior to the satellite era, unlike current approaches.

We employed multiple site-level observational data from the HadISD dataset to estimate EF_{SFE} and compared irrigated with nonirrigated regions in the CONUS. To control for confounding spatial and temporal differences in EF unrelated to irrigation, we further included EF from the ERA5 reanalysis (EF_{ERA5}) in this study. Irrigation is largely neglected in EF_{ERA5} due to the lack of irrigation schemes and interactive land-use changes in the reanalysis.

Using the available irrigation data, we tested five hypotheses (listed in section 2a) using the rationale outlined in Fig. 1. Consistent with hypothesis H1, EF_{SFE} is significantly higher at irrigated than at nonirrigated sites during droughts (Fig. 4). This difference between irrigated and nonirrigated regions is not significant outside periods of drought, which agrees with hypothesis H2. The differences are also not due to spatial differences in EF; if they were, they should be detectable in EF_{ERA5}, but they are not, consistent with hypothesis H3.

Our historical comparison between EF_{SFE} and EF_{ERA5} during droughts controls for changes in climate, and verifies hypotheses H4 and H5. The difference between changes in the two EFs from the 1970s to the 2000s is broadly consistent with the trends in proportion of county irrigated (Fig. 5). In regions where irrigation increased, EF_{SFE} also increased relative to EF_{ERA5} during meteorological droughts (Fig. 6), which is consistent with hypothesis H4. This shift in EF_{SFE} relative to EF_{ERA5} is not found in most regions without increasing irrigation (Fig. 7), which is consistent with hypothesis H5. Two exceptions are found in MO and ID; however, other irrigation-like modifications to the landscape at these sites likely explain the discrepancy.

Our study is subject to several limitations. We assume differences in EF_{SFE} and EF_{ERA5} are largely attributable to irrigation or other human interventions not included in the ERA5 reanalysis. However, at least some of the difference is likely due to errors in EF_{ERA5} and EF_{SFE}. Nonetheless, previous validation studies (McColl and Rigden 2020; Chen et al. 2021) provide some reason to expect that such errors do not dominate our analysis. It may be useful to examine other evapotranspiration products beyond ERA5 in future studies, but few ET products extend far enough back in time to be useful in studying the historical record of agricultural drought.

Our study is also limited by the availability of reliable irrigation data, resulting in small sample sizes, particularly in evaluating hypotheses H4 and H5. It may be useful to study factorial irrigation experiments in future studies, in which the irrigation signal can be cleanly isolated. However, such experiments would not provide information on the historical record.

In addition, while our analysis includes many of the most important regions where irrigation occurs in the United States, California's Central Valley was excluded due to limitations of SFE theory near coasts. We might expect hypothesis H2 to be rejected in this region since, in climatically drier regions like the Central Valley, there may still be differences in EF_{SFE} between irrigated and nonirrigated sites, even if the region is not technically in a drought. However, we do not see any reasons specific to the Central Valley that would cause the other hypotheses to be rejected.

Finally, the assumption used in SFE of no local advection may be violated to some extent near boundaries of irrigated regions, which can generate mesoscale circulations (Lo and Famiglietti 2013; Lo et al. 2021). However, the effects are typically not large enough to induce large errors in the SFE estimate, at least at the scales considered here. McColl and Rigden (2020) tested the theory at many sites across the inland continental United States, and around the world. While coastal regions were excluded, no other filtering was performed for spatial homogeneity, and most of the sites evaluated were spatially heterogeneous. The results found that, at a majority of sites, errors in the SFE predictions were similar to errors in the state-of-the-art eddy covariance observations used to test the theory, even after substantial quality control of the observations. While not all of these sites were irrigated, they included some irrigated regions, and all regions inevitably included other sources of heterogeneity. These results are further supported by Chen et al. (2021), who used a completely independent estimate of evaporation at larger spatial scales to reach a similar conclusion. We are not arguing that landscape heterogeneity, including that due to irrigation, does not induce mesoscale circulations and advection. We are simply arguing that, to the extent it exists, and induces errors in our approach, those errors are generally not large, at least in comparison to typical eddy covariance observation errors. Similar assumptions are also made in other approaches. For example, the ALEXI model (Anderson et al. 1997) relies on the boundary layer model of McNaughton and Spriggs (1986), and thus also implicitly assumes zero advection.

The approach described in this study can be used to study the role of irrigation on mitigating agricultural droughts in the historical record, particularly the presatellite era. There are surprisingly few alternative methods available for estimating EF during the presatellite era. Long-term records of EF from eddy covariance flux towers only date back to the 1990s. Estimates of EF using the Bowen ratio method require observations of air temperature and humidity at two different heights, yet standard weather stations typically only measure these quantities at one height (typically around 2 m above the ground). Approaches based on the complementary relationship (e.g., Kahler and Brutsaert 2006; Brutsaert 2015; Aminzadeh et al. 2016) provide an estimate of evapotranspiration, rather than EF. Converting the predicted evapotranspiration flux to EF would require observations of surface net radiation, which are also not widely available during the presatellite era. Thus, our approach fills an important methodological gap in the literature. We speculate that meteorological drought indices likely provide a distorted record of the relative severity of different agricultural droughts in the past, particularly after the advent of widespread irrigation following the Dust Bowl, and plan to use EF_{SFE} to reexamine the historical drought record.

Acknowledgments. K. A. M. acknowledges funding from NSF Grant AGS-2129576 and a Sloan Research Fellowship. Thanks to Andrew Feldman and two anonymous reviewers for constructive feedback.

Data availability statement. The gridded PDSI data (Dai et al. 2004) are available at https://climatedataguide.ucar.edu/climate-data/palmer-drought-severity-index-pdsi. HadISD data (Dunn et al. 2016) are available at https://www.metoffice.gov.uk/hadobs/hadisd/. ERA5 data are available at the ECMWF webpage. USDA census data can be downloaded from https://www.nass.usda.gov/AgCensus/index.php.

REFERENCES

AghaKouchak, A., A. Farahmand, F. S. Melton, J. Teixeira, M. C. Anderson, B. D. Wardlow, and C. R. Hain, 2015: Remote sensing of drought: Progress, challenges and opportunities. *Rev. Geophys.*, **53**, 452–480, https://doi.org/10.1002/2014RG000456.

Alley, W. M., 1984: The Palmer drought severity index: Limitations and assumptions. *J. Climate Appl. Meteor.*, **23**, 1100–1109, https://doi.org/10.1175/1520-0450(1984)023<1100:TPDSIL>2.0.CO;2.

Al-Yaari, A., A. Ducharne, W. Thiery, F. Cheruy, and D. Lawrence, 2022: The role of irrigation expansion on historical climate change: Insights from CMIP6. *Earth's Future*, **10**, e2022EF002859, https://doi.org/10.1029/2022EF002859.

Aminzadeh, M., M. L. Roderick, and D. Or, 2016: A generalized complementary relationship between actual and potential evaporation defined by a reference surface temperature. *Water Resour. Res.*, **52**, 385–406, https://doi.org/10.1002/2015WR017969.

Anderson, M. C., J. M. Norman, G. R. Diak, W. P. Kustas, and J. R. Mecikalski, 1997: A two-source time-integrated model for estimating surface fluxes using thermal infrared remote sensing. *Remote Sens. Environ.*, **60**, 195–216, https://doi.org/10.1016/S0034-4257(96)00215-5.

——, C. Hain, B. Wardlow, A. Pimstein, J. R. Mecikalski, and W. P. Kustas, 2011: Evaluation of drought indices based on thermal remote sensing of evapotranspiration over the continental United States. *J. Climate*, **24**, 2025–2044, https://doi.org/10.1175/2010JCLI3812.1.

Benjamini, Y., and Y. Hochberg, 1995: Controlling the false discovery rate: A practical and powerful approach to multiple testing. *J. Roy. Stat. Soc.*, **57B**, 289–300, https://doi.org/10.1111/j.2517-6161.1995.tb02031.x.

Brutsaert, W., 2015: A generalized complementary principle with physical constraints for land-surface evaporation. *Water Resour. Res.*, **51**, 8087–8093, https://doi.org/10.1002/2015WR017720.

Chen, F., W. T. Crow, R. Bindlish, A. Colliander, M. S. Burgin, J. Asanuma, and K. Aida, 2018: Global-scale evaluation of SMAP, SMOS and ASCAT soil moisture products using triple collocation. *Remote Sens. Environ.*, **214**, 1–13, https://doi.org/10.1016/j.rse.2018.05.008.

Chen, S., K. A. McColl, A. Berg, and Y. Huang, 2021: Surface flux equilibrium estimates of evapotranspiration at large spatial scales. *J. Hydrometeor.*, **22**, 765–779, https://doi.org/10.1175/JHM-D-20-0204.1.

Cook, E. R., R. Seager, M. A. Cane, and D. W. Stahle, 2007: North American drought: Reconstructions, causes, and consequences. *Earth Sci. Rev.*, **81**, 93–134, https://doi.org/10.1016/j.earscirev.2006.12.002.

Dai, A., K. E. Trenberth, and T. Qian, 2004: A global dataset of Palmer drought severity index for 1870–2002: Relationship with soil moisture and effects of surface warming. *J. Hydrometeor.*, **5**, 1117–1130, https://doi.org/10.1175/JHM-386.1.

Dunn, R. J. H., K. M. Willett, D. E. Parker, and L. Mitchell, 2016: Expanding HadISD: Quality-controlled, sub-daily station data from 1931. *Geosci. Instrum. Methods Data Syst.*, **5**, 473–491, https://doi.org/10.5194/gi-5-473-2016.

Evett, S. R., P. D. Colaizzi, F. R. Lamm, S. A. O'Shaughnessy, D. M. Heeren, T. J. Trout, W. L. Kranz, and X. Lin, 2020: Past, present, and future of irrigation on the U.S. Great Plains. *Trans. ASABE*, **63**, 703–729, https://doi.org/10.13031/trans.13620.

Hersbach, H., and Coauthors, 2020: The ERA5 global reanalysis. *Quart. J. Roy. Meteor. Soc.*, **146**, 1999–2049, https://doi.org/10.1002/qj.3803.

Hrozencik, R. A., and M. Aillery, 2021: Trends in us irrigated agriculture: Increasing resilience under water supply scarcity. USDA Rep. EIB-229, 55 pp., https://www.ers.usda.gov/webdocs/publications/102928/eib-229.pdf?v=5258.

Idaho Fish and Game, 2022: Fish hatcheries. State of Idaho, https://idfg.idaho.gov/visit/hatchery.

Kahler, D. M., and W. Brutsaert, 2006: Complementary relationship between daily evaporation in the environment and pan evaporation. *Water Resour. Res.*, **42**, W05413, https://doi.org/10.1029/2005WR004541.

Koster, R. D., and S. P. Mahanama, 2012: Land surface controls on hydroclimatic means and variability. *J. Hydrometeor.*, **13**, 1604–1620, https://doi.org/10.1175/JHM-D-12-050.1.

——, S. D. Schubert, and M. J. Suarez, 2009: Analyzing the concurrence of meteorological droughts and warm periods, with implications for the determination of evaporative regime. *J. Climate*, **22**, 3331–3341, https://doi.org/10.1175/2008JCLI2718.1.

Lo, M.-H., and J. S. Famiglietti, 2013: Irrigation in California's Central Valley strengthens the southwestern U.S. water cycle. *Geophys. Res. Lett.*, **40**, 301–306, https://doi.org/10.1002/grl.50108.

——, and Coauthors, 2021: Intense agricultural irrigation induced contrasting precipitation changes in Saudi Arabia. *Environ. Res. Lett.*, **16**, 064049, https://doi.org/10.1088/1748-9326/ac002e.

Lobell, D. B., and C. Bonfils, 2008: The effect of irrigation on regional temperatures: A spatial and temporal analysis of trends in California, 1934–2002. *J. Climate*, **21**, 2063–2071, https://doi.org/10.1175/2007JCLI1755.1.

Lu, J., G. J. Carbone, X. Huang, K. Lackstrom, and P. Gao, 2020: Mapping the sensitivity of agriculture to drought and estimating the effect of irrigation in the United States, 1950–2016. *Agric. For. Meteor.*, **292–293**, 108124, https://doi.org/10.1016/j.agrformet.2020.108124.

McColl, K. A., and A. J. Rigden, 2020: Emergent simplicity of continental evapotranspiration. *Geophys. Res. Lett.*, **47**, e2020GL087101, https://doi.org/10.1029/2020GL087101.

——, G. D. Salvucci, and P. Gentine, 2019: Surface flux equilibrium theory explains an empirical estimate of water-limited daily evapotranspiration. *J. Adv. Model. Earth Syst.*, **11**, 2036–2049, https://doi.org/10.1029/2019MS001685.

McLeman, R. A., J. Dupre, L. Berrang Ford, J. Ford, K. Gajewski, and G. Marchildon, 2014: What we learned from the Dust Bowl: Lessons in science, policy, and adaptation. *Popul. Environ.*, **35**, 417–440, https://doi.org/10.1007/s11111-013-0190-z.

McNaughton, K. G., and T. W. Spriggs, 1986: A mixed-layer model for regional evaporation. *Bound.-Layer Meteor.*, **34**, 243–262, https://doi.org/10.1007/BF00122381.

Mueller, N. D., E. E. Butler, K. A. McKinnon, A. Rhines, M. Tingley, N. M. Holbrook, and P. Huybers, 2016: Cooling of US Midwest summer temperature extremes from cropland intensification. *Nat. Climate Change*, **6**, 317–322, https://doi.org/10.1038/nclimate2825.

Munoz, S. E., and Coauthors, 2018: Climatic control of Mississippi River flood hazard amplified by river engineering. *Nature*, **556**, 95–98, https://doi.org/10.1038/nature26145.

Nocco, M. A., R. A. Smail, and C. J. Kucharik, 2019: Observation of irrigation-induced climate change in the Midwest United States. *Global Change Biol.*, **25**, 3472–3484, https://doi.org/10.1111/gcb.14725.

Palmer, W. C., 1965: Meteorological drought. U.S. Weather Bureau Research Paper 45, 58 pp., https://www.ncei.noaa.gov/monitoring-content/temp-and-precip/drought/docs/palmer.pdf.

Pinter, N., and R. A. Heine, 2005: Hydrodynamic and morphodynamic response to river engineering documented by fixed-discharge analysis, lower Missouri River, USA. *J. Hydrol.*, **302**, 70–91, https://doi.org/10.1016/j.jhydrol.2004.06.039.

Puy, A., and Coauthors, 2022: The delusive accuracy of global irrigation water withdrawal estimates. *Nat. Commun.*, **13**, 3183, https://doi.org/10.1038/s41467-022-30731-8.

Raghav, P., and M. Kumar, 2021: Retrieving gap-free daily root zone soil moisture using surface flux equilibrium theory. *Environ. Res. Lett.*, **16**, 104007, https://doi.org/10.1088/1748-9326/ac2441.

Salvucci, G. D., and P. Gentine, 2013: Emergent relation between surface vapor conductance and relative humidity profiles yields evaporation rates from weather data. *Proc. Natl. Acad. Sci. USA*, **110**, 6287–6291, https://doi.org/10.1073/pnas.1215844110.

Seager, R., Y. Kushnir, C. Herweijer, N. Naik, and J. Velez, 2005: Modeling of tropical forcing of persistent droughts and pluvials over western North America: 1856–2000. *J. Climate*, **18**, 4065–4088, https://doi.org/10.1175/JCLI3522.1.

Seneviratne, S. I., T. Corti, E. L. Davin, M. Hirschi, E. B. Jaeger, I. Lehner, B. Orlowsky, and A. J. Teuling, 2010: Investigating soil moisture–climate interactions in a changing climate: A review. *Earth Sci. Rev.*, **99**, 125–161, https://doi.org/10.1016/j.earscirev.2010.02.004.

Thenkabail, P. S., and Coauthors, 2009: A Global Irrigated Area Map (GIAM) derived from remote sensing, for the end of the last millennium. *Int. J. Remote Sens.*, **30**, 3679–3733, https://doi.org/10.1080/01431160802698919.

USDA National Agricultural Statistic Service, 2022: Census of agriculture. https://www.nass.usda.gov/AgCensus/index.php.

Vicente-Serrano, S. M., and Coauthors, 2012: Performance of drought indices for ecological, agricultural, and hydrological applications. *Earth Interact.*, **16**, https://doi.org/10.1175/2012EI000434.1.

Wilks, D. S., 2016: "The stippling shows statistically significant grid points": How research results are routinely overstated and overinterpreted, and what to do about it. *Bull. Amer. Meteor. Soc.*, **97**, 2263–2273, https://doi.org/10.1175/BAMS-D-15-00267.1.

Woodhouse, C. A., and J. T. Overpeck, 1998: 2000 years of drought variability in the central United States. *Bull. Amer. Meteor. Soc.*, **79**, 2693–2714, https://doi.org/10.1175/1520-0477(1998)079<2693:YODVIT>2.0.CO;2.

Worster, D., 2004: *Dust Bowl: The Southern Plains in the 1930s*. Oxford University Press, 304 pp.

Supplemental Material

Journal of Hydrometeorology
An Observational, Irrigation-Sensitive Agricultural Drought Record from Weather Data
https://doi.org/10.1175/JHM-D-23-0026.1

Supplemental Materials for "An Observational, Irrigation-sensitive Agricultural Drought Record from Weather Data"

Lois I. Tang[a] and Kaighin A. McColl[a,b]

[a] *Department of Earth and Planetary Sciences, Harvard University, Cambridge, Massachusetts.*

[b] *School of Engineering and Applied Sciences, Harvard University, Cambridge, Massachusetts.*

Corresponding author: Lois I. Tang, loistang@fas.harvard.edu

Table S1. Table of irrigated sites in HadISD data. Format of time: MM/DD/YY.

site	latitude	longitude	county	state	start time	end time
ID	44.021	-117.013	Malheur	OR	01/01/48	present
	43.567	-116.241	Boise	ID	01/01/31	present
	43.05	-115.867	Elmore	ID	01/01/32	3/27/19
	42.483	-114.483	Twin Falls	ID	01/01/73	present
	42.542	-113.766	Cassia	ID	1/01/48	present
	42.92	-112.571	Power	ID	01/01/43	present
	43.519	-112.064	Bonneville	ID	01/01/48	present
	43.832	-111.808	Madison	ID	01/02/99	present
NE	40.450	-99.333	Phelps	NE	01/01/73	present
	40.717	-99.000	Buffalo	NE	03/12/43	present
	40.605	-98.428	Adams	NE	01/01/73	present
	40.961	-98.314	Hall	NE	03/01/44	present
	41.986	-97.435	Madison	NE	01/01/48	present
	41.450	-97.333	Platte	NE	01/01/73	present
	40.300	-96.750	Gage	NE	01/01/73	present
	40.851	-96.748	Lancaster	NE	10/01/42	present
MS	35.056	-89.987	Shelby	TN	10/01/46	present
	35.967	-89.950	Mississippi	AR	09/01/42	present
	35.350	-89.867	Shelby	TN	03/01/45	12/31/04
	34.180	-91.934	Jefferson	AR	01/01/73	present
	36.125	-90.925	Lawrence	AR	10/10/42	present
	35.833	-90.633	Craighead	AR	01/01/73	present
	36.767	-90.467	Butler	MO	08/20/76	12/31/05
	33.483	-90.985	Washington	MS	01/20/42	present
KT	36.017	-102.550	Hartley	TX	11/01/42	present
	33.600	-102.050	Lubbock	TX	03/01/42	05/01/97
	33.666	-101.823	Lubbock	TX	08/10/45	present
	35.230	-101.704	Potter	TX	03/01/43	present
	37.033	-100.95S	Seward	KS	06/18/43	present
	37.927	-100.725	Finney	KS	02/01/43	present
	37.769	-99.968	Ford	KS	04/19/43	present

Table S2. Table of nonirrigated sites in HadISD data. Format of time: MM/DD/YY. * Cibola, NM used to be a part of Valenncia, NM. For consistency, we eliminated this county for the total irrigated area in USDA census.

site	latitude	longitude	county	state	start time	end time
SD	46.783	-100.757	Burleigh	ND	07/01/36	present
	45.547	-100.408	Walworth	SD	01/01/73	present
	44.381	-100.286	Hughes	SD	03/01/44	present
	43.800	-99.317	Brule	SD	03/10/78	present
	46.926	-98.669	Stutsman	SD	12/01/48	present
	45.443	-98.413	Brown	SD	01/01/48	present
	44.398	-98.223	Beadle	SD	01/01/40	present
	43.775	-98.039	Davison	SD	01/01/73	present
MO	37.152	-94.495	Jasper	MO	01/01/48	present
	36.917	-94.017	Barry	MO	01/01/73	present
	37.240	-93.390	Greene	MO	01/01/48	present
	38.717	-93.550	Buchanan	MO	12/01/42	present
	38.817	-92.218	Boone	MO	11/01/69	present
	37.750	-92.150	Pulaski	MO	03/20/63	present
	38.583	-92.150	Cole	MO	11/29/73	present
	38.131	-91.768	Carter	MO	01/01/48	present
NM	37.300	-108.633	Montezuma	CO	01/01/73	present
	36.744	-108.229	San Juan	NM	01/01/49	present
	35.514	-108.794	McKinley	NM	01/01/73	present
	35.165	-107.902	Cibola*	NM	01/01/48	present
	35.879	-106.269	Los Alamos	NM	02/28/80	present
	35.617	-106.089	Santa Fe	NM	08/01/46	present
	35.654	-105.142	San Miguel	NM	08/01/46	present
KY	35.951	-85.081	Cumberland	TN	05/01/54	present
	38.041	-84.606	Fayette	KY	01/01/48	present
	37.087	-84.077	Laurel	KY	10/11/54	present
	35.818	-83.986	Blount	TN	01/01/48	present
	37.591	-83.314	Breathitt	KY	01/02/73	present
	35.432	-82.538	Bumcombe	NC	08/01/43	present
	36.473	-82.404	Sullivan	TN	01/01/48	present

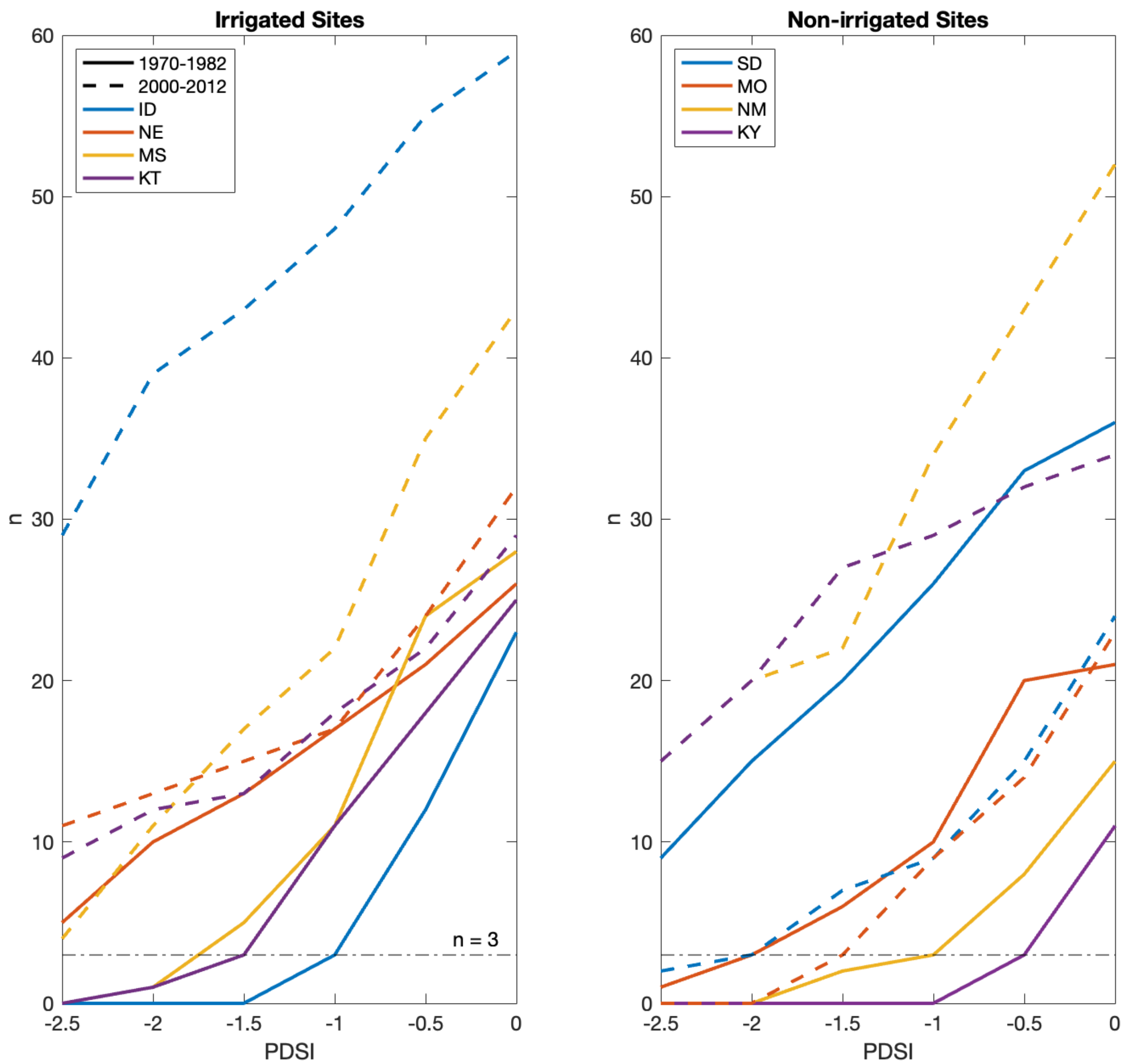

Fig S1. Sample size of data discussed in section 3b of the main text when using different PDSI thresholds to define a drought: the left panel shows the sample size (n) at irrigated sites, and the right panel shows n at nonirrigated sites. Solid lines indicate the period of 1970-1982, and dashed lines are for 2000-2012, with colors indicating different sites.

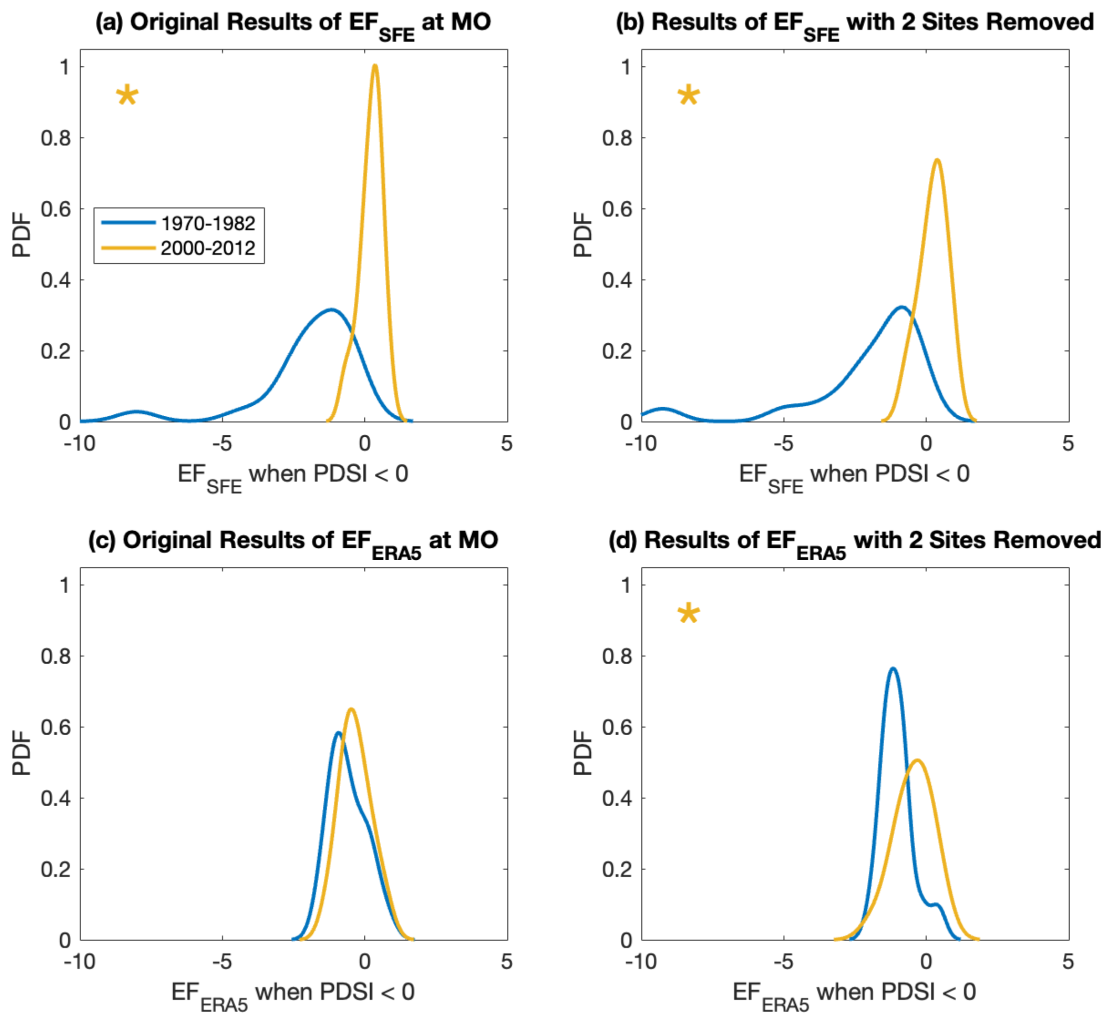

Fig S2. The original distribution of EF_{SFE} (panel (a)) and EF_{ERA5} (panel (c)) at MO when PDSI is negative (Figs. 7 (d) and (i) of the main text). Panels (b) and (d) respectively show the corresponding results with the two sites along the lower Missouri river (in Boone county and Cole county, MO) removed. Panels with an asterisk (*) on the upper left indicate results with 2000-12 greater than 1970-82 with statistical significance. This figure shows that after the removal of two sites closest to the river, changes in EFs at MO are consistent with our hypothesis that the trends in EF_{SFE} and EF_{ERA5} are consistent when PDSI is negative.